Anharmonic Vibrational Spectroscopy Calculations for Proton-Bound Amino Acid Dimers[†]

Adeyemi A. Adesokan[‡] and R. B. Gerber*[,‡,§]

Department of Chemistry, University of California at Irvine, Irvine, California 92697, and Department of Physical Chemistry and The Fritz Haber Research Center, The Hebrew University of Jerusalem, Jerusalem 91904, Israel

Received: August 8, 2008; Revised Manuscript Received: October 28, 2008

Results of anharmonic frequency calculations carried out for $GlysLysH^+$ and $GlyGlyH^+$ are presented and compared to gas phase electrospray ionization (ESI) spectroscopy experiments. Anharmonic frequencies are obtained via correlation-corrected vibrational self-consistent field (CC-VSCF) calculations. The potential used is based on the PM3 semiempirical electronic structure method, but improved by fitting to ab initio MP2 calculations at the harmonic level. The key results are as follows: (1) Hydrogens acting as intermolecular bridges have very anharmonic stretches whose frequencies cannot be reliably predicted by the harmonic approximation. An example is the carboxylate bound NH_3^+ stretch. (2) The computed anharmonic vibrational frequencies are in good agreement with experiment and provides a very large improvement over harmonic frequencies especially for OH and NH stretches. For example the calculated CC-VSCF frequencies of $GlysLysH^+$ and $GlyGlyH^+$ have overall average deviations of 1.35% and 1.48% only, respectively, from experiment. (3) The harmonic OH bond stretching frequency deviates by 6.64% from experiments. The CC-VSCF calculations reduce this deviation by more than an order of magnitude to 0.56%. The anharmonicity of the OH stretch is intrinsic, rather than due to coupling with other modes. (4) Anharmonic coupling between the NH_3^+ stretch and several other normal modes is strong, and provide the main contribution for the anharmonicity of this mode. Properties of the potential energy surfaces of the proton-bound complexes are briefly discussed in light of the results.

1. Introduction

There has been great progress in recent years in experimental studies of biological molecules in the gas phase. Mass spectrometric techniques and vibrational spectroscopy, often in a combined framework, have been the main experimental tools in this area.[1−23] These experiments have provided unprecedented insight into the mechanisms underlying fundamental biological processes such as protein folding, enzyme substrate binding, nucleic acid tautomerization and base pairing.[24−29] Experimental spectroscopic techniques that have been recently applied to the study of fairly large biological molecules include electrospray ionization techniques (ESI)[30] and matrix assisted laser desorption ionization (MALDI),[31] infrared photo dissociation techniques (IRPD).[32−34] The application of sensitive IRPD to isolated and microsolvated protonated peptides and proton bound dimers of amino acids has provided useful information on the dissociation behavior, preferred protonation sites and the influence of solvation in nonpolar environments.[32−35] Similarly, the development and appreciation of the ESI methodology makes possible the efficient ionization of biomolecules as large as ubiquitin[30] and has thus provided unique information on noncovalent bonding of OH and NH groups especially when applied microsolvated proton clusters such as $(H_2O)_2$-$8H^+$ and water bound ammonium clusters such as $(H_2O)_3$-$6(NH_4^+)$.[36−40]

Proton bound dimers have been a subject of extensive research by mass spectrometry methods especially those focused on the determination of proton affinities and bond dissociation energies.[41] More light has been shed on questions regarding the structural effects of competitive charging of heteroatoms,[42] factors necessary for the stabilization of gas phase zwitterionic species[42,43] through spectroscopic studies on proton bound amino acid dimers.

Vibrational spectroscopy as a structural tool has been used to characterize the structure of cationized amino acids in the gas phase. Kapota et al.[44] were able to probe the structure of sodiated glycine and proline, yielding infrared signatures of nonzwitterionic and zwitterionic forms respectively, of cationized aliphatic amino acids. Vibrational spectroscopy can be used as a probe of the molecular properties of biomolecules as it is sensitive to the potential energy surface (PES). In this respect, the method has an important advantage. Coupling between normal modes arises only beyond the harmonic level, so anharmonic vibrational calculations are able to provide insight into energy flow patterns between the normal modes of vibration. Thus it is evident that anharmonic calculations not only can validate the PES but also can provide information on processes, such as energy flow between vibrational modes. Little is known of the structures of the proton-bound species, and this information is potentially biologically important.

In this paper we present a computational study of the anharmonic vibrational spectroscopy of two proton bound amino acid wires, $GlyGlyH^+$ and $GlyLysH^+$, by means of the correlation-corrected variant of the vibrational self-consistent field (CC-VSCF) method.[45−52] The main objective is to test potential surfaces for these systems against spectroscopic data, and also to analyze some properties of the potentials. In this framework, agreement between calculations and experiment, if found (as is the case) here also supports the computed structure. The calculations are for a multidimensional potential energy surface (PES) of a semi empirical electronic structure theory improved

[†] Part of the "Max Wolfsberg Festschrift".
[‡] University of California at Irvine.
[§] The Hebrew University of Jerusalem.

10.1021/jp807106h CCC: $40.75
Published on Web 12/05/2008

by input from high level ab initio calculations. The advantages of applying the CC-VSCF method to these proton bound amino acid dimers includes the following: (a) The method has been proven to be of good accuracy when applied to a range of realistic systems. (b) CC-VSCF directly employs potentials obtained from electronic structure theory. (c) Computationally, the method can be applied, with suitable potentials, for large systems as pertinent for the present applications.

The outline of this paper is as follows: In the Methodology section we present an overview of the VSCF method. In the Results and Discussion section, we consider the molecular geometry of the systems studied and also present a comparison of theory with experiment. We focus particularly on the evaluation and properties of the high-level semiempirical surfaces used. This is followed by comments on the difference between the PES of $GlyGlyH^+$ and $GlyLysH^+$ and the anahrmonic effects in the systems studied. Finally, we close with concluding remarks on the need for accurate anharmonic calculations to complement advances in experimental spectroscopic methods in connection with dynamical properties of the systems, including propensities for intramolecular vibrational energy flow and for proton transfer processes.

2. Methodology

2.1. The Vibrational Self-Consistent Field Method (VSCF). Anharmonic interactions, including coupling between different modes, were treated in this study by the use of the VSCF approach and its variants.[45,49] These methods are currently implemented in the GAMESS suite of codes, and the calculations carried out here used this package.[53] This algorithm can be directly applied to potential surfaces from electronic structure methods, and a range of previous applications has shown it to be reasonably accurate for numerous systems, including amino acids and their hydrogen-bound complexes.[46−52] Unlike analytic force fields, the potential surface is generated on grid points and is not available as an analytic function. Since VSCF has been discussed extensively in the literature, here we have only a brief overview of the method.[46−51]

The VSCF method is used to solve the vibrational Schrödinger equation to obtain vibrational wave functions in mass-weighed normal coordinates. At the lowest level, VSCF is a separable but anharmonic approximation. The vibrational wave functions are computed from mean-field potentials that represent the effects of the other vibrations on a given mode. The correlation-corrected VSCF (CC-VSCF) algorithm,[45] which is the variant used here, goes beyond separability of the normal modes, by applying second-order perturbation theory to the lowest-level VSCF approximation. This variant of the method has been extensively tested, with satisfactory results, for a range of biological molecules including amino acids.[47,48]

Variants of VSCF were developed to treat degeneracy or near-degeneracy effects. These include VCI (vibrational configuration interaction) and VSCF-DPT (VSCF with degenerate perturbation theory).[49] VCI includes degeneracies at the level of 1:1 resonances. VSCF-DPT2 corrects VCI by second-order perturbation theory.

Practically, the main computational difficulty in VSCF involves numerical solutions of costly multidimensional integrals. Following refs 45 and 48, we have found it advantageous to represent the potential as a sum of terms that includes single-mode potentials $V_j^{\mathrm{diag}}(Q_j)$, and interactions between pairs of normal modes $W_{ij}^{\mathrm{coup}}(Q_i,Q_j)$. Contributions to the potential from interactions of triplets and quartets (or higher order interactions) of normal modes are neglected and the potential is thus written as

$$V(Q_1,...,Q_N)=\sum_{j=1}^{N} V_j^{\mathrm{diag}}(Q_j)+\sum_i\sum_{j>i} W_{ij}^{\mathrm{coup}}(Q_i,Q_j) \quad (1)$$

Although this approximation has proven to be successful in many cases, it cannot be taken for granted and must be tested for each application.[46] Cases where couplings between triplets of normal modes are important were found. This is the case with mode characterized by soft, large amplitude torsional motions.[54]

Two types of anharmonic interactions are thus taken into account in the VSCF framework: (1) the intrinsic anharmonicity which is given by the single mode or diagonal potentials and does not involve coupling with other modes and (2) anharmonicity due to the mode−mode coupling.

2.2. Potential Functions. Anharmonic vibrational spectroscopy calculations were carried out on an improved semi empirical (PM3) potential energy surface (PES).[47] PM3 is one of several modified NDDO approximations methods (neglect of diatomic differential overlaps methods).[55] However, while computationally efficient, standard PM3 is not sufficiently accurate. Our approach in improving PM3 in this context was originally proposed and implemented for a large range of biomolecules by Brauer et al.[47] and has been validated by subsequent studies.[50] The method involves changing the harmonic force constants so as to agree with harmonic force constants obtained from a reliable ab initio method. The (improved) PM3 level is designed to agree with the MP2 level at the harmonic approximation. This is accomplished by introducing a scaling of PM3, such that

$$V_{\mathrm{scaled}}(Q_1,...,Q_n)=V_{\mathrm{PM3}}(\lambda_1 Q_1,...,\lambda_n Q_n) \quad (2)$$

where V_{scaled} is a scaled potential, V_{PM3} is the PM3 potential surface and Q_j is the jth normal mode coordinate. The scale factor λ_j is determined by the ratio

$$\lambda_i=\omega_{\mathrm{MP2},i}/\omega_{\mathrm{PM3},i} \quad (3)$$

where $\omega_{\mathrm{MP2},i}$ is the ith harmonic frequency obtained by the MP2 method, while $\omega_{\mathrm{PM3},i}$ represents the corresponding harmonic frequency obtained by PM3. The λ_i factors were then entered into the potential surface calculation in the VSCF portion of the GAMESS program. Thus, the standard PM3 potential surface in normal coordinates is modified by scaling of each mode coordinate Q_j with the scale factor λ_i. While the scaling is expected to improve the potential at the harmonic level, since MP2 is superior to standard PM3, the effect of the scaling beyond this approximation can only be tested by the predictions obtained with the scaled potential.

The preconditions for carrying out this scaling procedure include similarities in the MP2 and PM3 structures, and a close correspondence in the nature of the vibrational modes that are being scaled. The proposed scaling makes intuitive sense only if the PM3 normal mode being scaled is similar to the MP2 mode used in scaling. As a test of similarity, a one-to-one correspondence between the normal modes from the two methods were obtained mainly via visual comparison using the MacMolPlt program.[56]

3. Results and Discussion

3.1. Molecular Geometry. Calculations for both proton bound amino acid dimers were based on the minimum energy structure deduced by MP2/DZP calculations and by semiempirical methods. Figures 1 and 2 show the structures of $GlyLysH^+$ and $GlyGlyH^+$ while Figure 3 shows a representative atom numbering scheme for $GlyGlyH^+$. On comparison, the

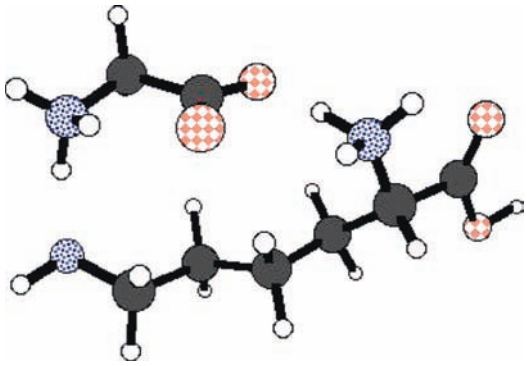

Figure 1. Equilibrium structure of GlyLysH$^+$.

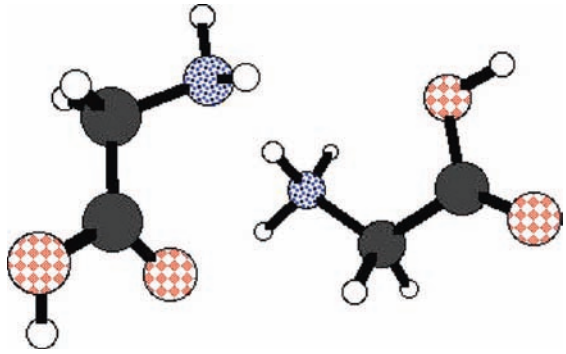

Figure 2. Equilibrium structure of GlyGlyH$^+$.

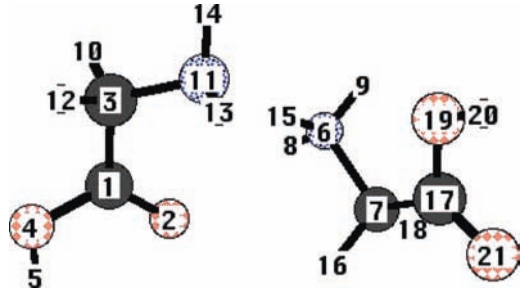

Figure 3. Equilibrium structure and numbering scheme of GlyGlyH$^+$.

bond lengths and bond angles obtained theoretically via MP2 methods are in agreement with earlier studies. Also for both systems we observe good agreement between ab intio and PM3 calculated bond distances.

Figure 2 shows a proton bridge between the glycines through an extra proton on N6. There is an extra proton on the nitrogen next to the carbonyl carbon on lysine; this extra proton provides a bridge linking the oxygen on the glycine.

3.2. Vibrational Frequencies: Comparison of Theory and Experiment. The anharmonic vibrational frequencies of the normal modes of vibration of GlyGlyH$^+$ and GlysLysH$^+$ were calculated by means of the CC-VSCF method and compared to experimental frequencies, harmonic frequencies and IRPD experiments.

***A. GlysLysH*$^+$.** Generally the CC-VSCF calculations carried out for GlysLysH$^+$ had an overall deviation of about 1.35% from experiments with a major portion of the species having a deviation of less than 1% from IRPD experimental frequencies (Table 1). We note the power of VSCF and implicitly also that of the pairwise mode−mode coupling approximation used. Particularly, excellent results are observed for the OH stretch where a deviation of 0.56% is observed in comparison of VSCF results to experiment. This is the case also for the NH stretch

TABLE 1: GlyLysH$^+$ Assignment and Comparison of Theoretical Harmonic and Anharmonic Frequencies in Wave Numbers to Those Obtained from Experiments

PM3 mode	harmonic (MP2/DZP)	CC-VSCF (imp. PM3)	IRPD	mode description
1	3822	3564	3584	OH stretch
2	3598	3475	3470	NH stretch
3	3488	3488	3426	NH_3^+ stretch
4	3526	3242	3410	NH_3^+ stretch
5	3393	3393	3371	NH_3^+ stretch
6	3619	3300	3300	NH_3^+ stretch
7	3147	3147	3138	NH_3^+ stretch

TABLE 2: GlyGlyH$^+$ Assignment and Comparison of Theoretical Harmonic and Anharmonic Frequencies in Wave Numbers to Those Obtained from Experiments

PM3 mode	harmonic (MP2/DZP)	CC-VSCF (imp. PM3)	IRPD	mode description
1	3839	3574	3584	OH stretch
2	3785	3562	3584	OH stretch
3	3544	3261	3372	NH_3^+ sym stretch
4	3531	3296	3400	NH sym stretch
5	3191	3045	3045	CH sym stretch
6	3151	3009	3000	CH asym stretch
7	3285	2958	3042	CH asym stretch

where a deviation of 0.14% is observed. The best results observed for GlyLysH$^+$ are seen on the NH_3^+ stretch where scaled VSCF predicts the frequency of this mode exactly at 3300 cm^{-1}. This shows the inherent accuracy of the scaled PM3 surface in the description of the vibrational spectra of charged complexes. The VSCF errors occur in the range of 0 cm^{-1} to 168 cm^{-1}. The mean harmonic deviation for the GlyLysH$^+$ complex is 4.2% with the largest harmonic deviation of about 319 cm^{-1}.

The experimental method used (IRPD) can only determine frequencies in the range of hydrogenic stretches. CC-VSCF results are available for all fundamental transitions (though not listed here), and hopefully future experiments will make possible tests of the calculations also for the lower frequency. However, already at this stage, the agreement for the hydrogenic stretch region is very encouraging, and strongly supports the structure computed for the GlyLysH$^+$ species.

***B. GlyGlyH*$^+$.** An overall mean deviation of about 1.48% from the experimental frequencies for GlyGlyH$^+$ was observed with a majority of the modes having a deviation of less than 0.7% (see Table 2). Similar to GlyLysH$^+$ the best CC-VSCF results where for the OH stretch. For mode number 1 (OH stretch), a percentage deviation of 0.28% from experiment is observed compared to harmonic at 7.01%. CC-VSCF performed well also for mode number 2, where a percentage deviation of 0.6% was observed. With the application of the CC-VSCF method the NH_3^+ symmetric stretch showed a deviation of 3.2% from experiment compared to the harmonic frequency at 5.01%. All the CH stretches showed excellent agreement with experiment. For the CH stretch modes, the average overall deviation of about 1% was observed when compared to experiment. Particularly, CC-VSCF calculations for the CH symmetric stretch (3045 cm^{-1}) showed a deviation of 0.07% from experiment. The CH symmetric stretch for the stretch at 3000 cm^{-1} showed a deviation of about 0.38% from experiment.

CC-VSCF frequency errors for GlyGlyH$^+$ are in the range of 18 cm^{-1} to 121 cm^{-1} with the highest CC-VSCF error being for the NH_3^+ asymmetric stretch. This may be due to errors in the PM3 description of charged complexes. The largest harmonic

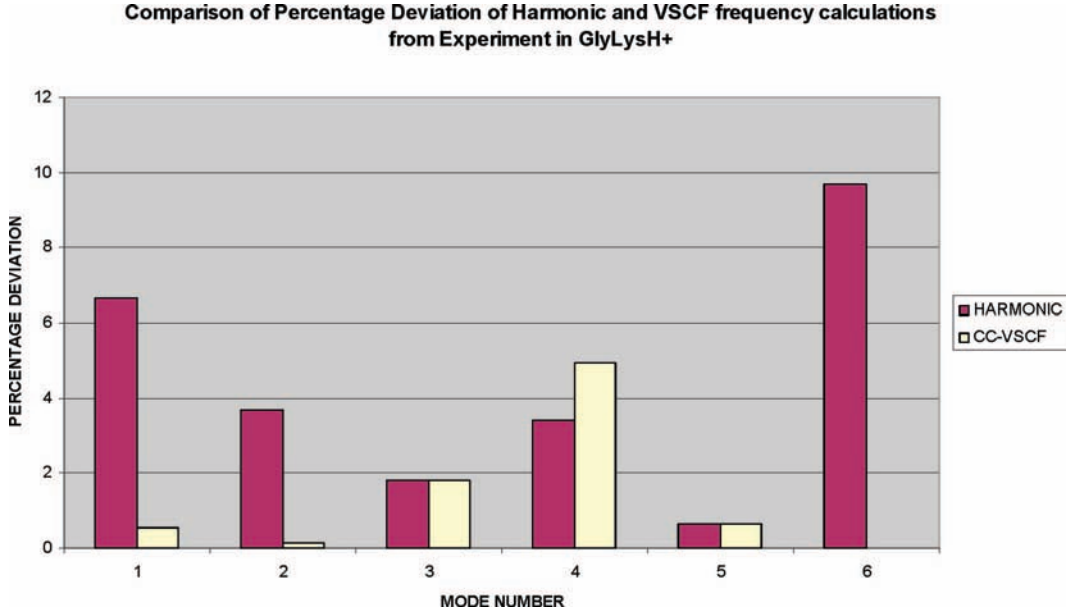

Figure 4. $GlyLysH^+$: theory vs experiment. The CC-VSCF anharmonic frequency in mode 6 shows a 0% deviation from experiment.

deviation was at 245 cm^{-1} for the CH asymmetric stretch. Upon comparison the OH stretch gave the best agreement with experiment while the NH_3^+ asymmetric stretch gave the highest deviation form experiment. As will be seen below, the anharmonic effects for the OH stretch are mostly due to the intrinsic potential of the mode, while in the case of NH_3^+ the effect is mostly due to coupling with other modes. It is plausible that the results are slightly less successful for NH_3^+ because PM3 is less accurate for mode−mode coupling.

Difficulties with the use of PM3 for describing hydrogen bonded complexes have been discussed by several authors and have been attributed to the inadequate description of the rotational barriers of the amide bond by PM3.[56,57] The impact of errors due to PM3 are however reduced, through the application of ab initio scaling methods to PM3, as the predictions are quite satisfactory, if not completely accurate.

C. Functional Group Effects. In this section we consider how well CC-VSCF represents important functional group effects of the proton bound amino acid dimers. Earlier work by Oh et al.[17] has shown the frequencies of the OH and NH stretches, the major functional groups responding in the 3050−3800 cm^{-1} region, are weakened and the frequencies are lowered by hydrogen bonding and by an electron withdrawing group or a partial positive charge on the heteroatom. In the present calculations, CC-VSCF proved to be able to adequately predict the frequencies of the OH stretch modes, an important functional group in both $GlyGlyH^+$ and $GlyLysH^+$. It has also been noted by Oh et al. that, for primary amines in solution, the free N−H symmetric and asymmetric stretches are at ∼3400 cm^{-1} and ∼3500 cm^{-1}, respectively, and their gaseous counterparts are weak and difficult to assign without theory. Earlier theoretical work shows the symmetric NH_3^+ stretch at 3375 cm^{-1} and the NH stretch at 3400 cm^{-1}. In the present calculations,[17]

CC-VSCF were able to reproduce this pattern with a prediction of 3261 for the NH_3^+ stretch and 3296 cm^{-1} for the NH stretch.

In earlier work by Oh et al.[17] it is noted that hydrogens acting as intermolecular bridges between and ammonium ion and a carboxylate ion are likely to have very anharmonic stretches whose frequencies cannot be predicted reliably by the harmonic approximation.[17] The NH_3^+ stretch toward the carboxylate oxygen is a particular case. However most of these stretches are outside of the IRPD range. An examination of this interaction and the anharmonic prediction for it will thus have to await future experimental tests.

The available comparison with experiment on the spectra of the functional groups leads to the following observation: Anharmonic effects included in the calculations clearly improve agreement with experiment quite significantly. At the same, such agreement is sensitive to the positions of the functional groups within the complex, and therefore to the structure of the complex. This is therefore an important role for anharmonic calculations in determining or analyzing the structure of protein bridges.

3.3. Nature of Anharmonic Effects. ***A. Comparison of CC-VSCF and Harmonic Frequency Deviations.*** Figures 4 and 5 show a comparison of percentage deviations from experiment for the calculated CC-VSCF anharmonic frequencies and also percentage deviations of the MP2 harmonic frequencies for the proton and amino acid dimmers. The advantage of CC-VSCF in applying the anharmonic correction is dramatic for the OH stretch mode where the harmonic approximation produces an error of 6.6% compared to CC-VSCF at 0.56%. This is also the case with the NH stretch mode where the harmonic approximation gave an error of 3.69% compared to CC-VSCF at 0.14%. The advantage of CC-VSCF is highlighted the most in mode 6 (NH_3^+) of $GlyLysH^+$, where the harmonic approximation resulted in a deviation of 9.67% compared to an "exact" description by CC-VSCF. The use of the anharmonic correction proves necessary for the OH stretch as a correction of 7.11% harmonic to 0.28% anharmonic is observed. For the other OH stretch, a 5.6% harmonic approximation compared to 0.6% anharmonic for the OH stretch is observed. These especially large corrections are characteristic of the hydrogen bonded stretch modes and can be attributed to the high anharmonicity inherent in hydrogen bonded complexes. We did not attempt in this work to apply (empirical) anharmonic scaling factors to the ab initio harmonic calculations, as is often practiced. While such an approach often gives very good

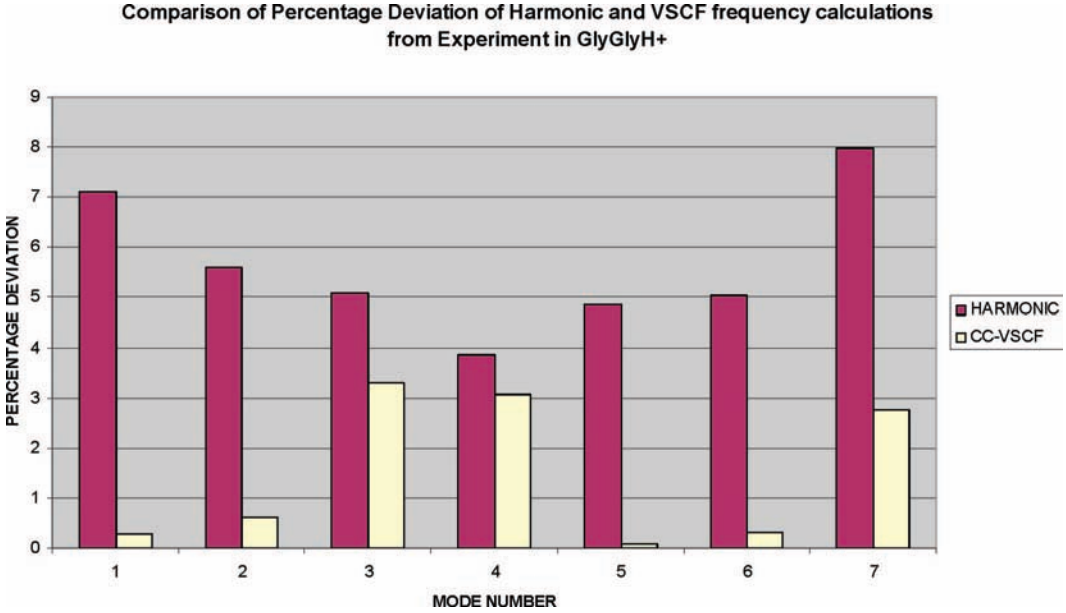

Figure 5. $GlyGlyH^+$: theory vs experiment.

TABLE 3: $GlysLysH^+$: Comparison between ΔE_{diag} (in cm^{-1}) and ΔE_{coup} (in cm^{-1})

PM3 mode	MP2 (harm.)	diag freq	CC-VSCF (ab initio)	IRPD (exp)	$\lvert\Delta E\rvert_{diag}$	$\lvert\Delta E\rvert_{coup}$
1	3822	3570	3574	3584	252	4
2	3598	3393	3475	3470	205	82
3	3488	3256	3488	3426	232	232
4	3526	3350	3242	3410	176	108
5	3393	3300	3393	3371	393	93
6	3619	3515	3300	3300	104	215

TABLE 4: $GlyGlyH^+$: Comparison between ΔE_{diag} (in cm^{-1}) and ΔE_{coup} (in cm^{-1})

PM3 mode	MP2 (harm.)	diag freq	CC-VSCF (ab initio)	IRPD (exp)	$\lvert\Delta E\rvert_{diag}$	$\lvert\Delta E\rvert_{coup}$
1	3839	3619	3574	3584	220	45
2	3785	3603	3562	3584	182	41
3	3544	3434	3261	3372	110	173
4	3531	3441	3296	3400	90	145
5	3191	3171	3045	3045	20	126
6	3151	3112	3009	3000	39	103
7	3285	3251	2958	3042	34	293

agreement with experiment, it does not provide any insight to the role and nature of the anharmonicities of the potential surface.

B. Comparison of Intrinsic and Coupling Anharmonicities. As mentioned previously, there are two different causes of anharmonic effects, the intrinsic anharmonicity of the individual modes and the anharmonic coupling between different modes. The contribution of the intrinsic single mode anharmonicty (ΔE_{diag}) to the frequency is calculated as the difference between the frequency given by the diagonal potential $V_j^{diag}(Q_j)$ and the harmonic value of the frequency. On the other hand, the contribution of the anharmonic coupling element between modes (ΔE_{coup}) is computed as the difference between the CC-VSCF value and the frequency value given by $V_j^{diag}(Q_j)$.

Here we compare the values of ΔE_{diag} and ΔE_{coup}.

For $GlysLysH^+$ the absolute value of ΔE_{diag} is higher than that of ΔE_{coup} for most of the vibrational modes (Table 3). This indicates that for these degrees of freedom the contribution from single mode anharmonicities is greater than anharmonic coupling between modes. The exception to this pattern in $GlysLysH^+$ are modes 3 and 6 which represent NH_3^+ coupling to a carboxylate group. For $GlyGlyH^+$ the contributions of coupled anharmonicity seem to be higher than those of single mode anharmonicities for most transitions (Table 4). The absolute value of ΔE_{coup} is higher in modes 3, 4, 5,6 and 7, while ΔE_{diag} is higher for modes 1, 2 and 3. Modes 5, 6 and 7 in $GlyGlyH^+$ are aliphatic CH bond stretches, and we observe that the attributed anharmonicity is mostly due to coupling. On the other hand we observe that the anharmonicities due to the OH and NH stretches are mostly intrinsic. Hence we see a similarity in the intrinsic anharmonic character of the OH stretches in both $GlyLysH^+$ and $GlyGlyH^+$. In dynamics, the anharmonic coupling between different normal modes is the driving force for intramolecular vibrational energy flow. Thus, the above analysis suggests that in $GlyLysH^+$, vibrational energy flow from modes of NH_3^+ at the carboxylate should be efficient. On the other hand, vibrational excitation of the OH stretch should not be especially of a short lifetime since the anharmonicity of this mode, while high, does not involve strong coupling with other modes. Also, an obvious corollary of the above analysis is that in dynamics, the $GlyGlyH^+$ should exhibit faster intramolcular vibrational redistribution than $GlyLysH^+$.

C. Magnitude of Anharmonic Coupling between Modes. Analysis of pairwise coupling effects in proton wires may provide some insights into the nature of vibrational energy flow in amino acids and peptides.[58] Specifically, this can yield useful information on the pairs of normal modes that are expected to be important in vibrational energy transfer. This is examined here for $GlysLysH^+$, using the mean absolute value potentials, which are generated in the CC-VSCF algorithm. Generally, we observe coupling is strongly mode-selective.

In the case of the OH stretch (mode 1) in $GlysLysH^+$ there is a very small coupling observed (Figure 6). This supports the study in the previous section which shows the anharmonicity in the OH stretch in $GlysLysH^+$ have a very intrinsic character (Table 3). For the NH_3^+ (mode 3) stretch in $GlysLysH^+$, however, very strong coupling of this mode is observed however with mode 2 and mode 7 (NH_3^+ stretches toward the carboxylate) (Figure 7). This coupling is due to the interaction of the NH stretch mode with the other hydrogens bound to the N2. Another interesting case is seen in the carboxylate bound NH_3^+ stretch in $GlysLysH^+$ where the

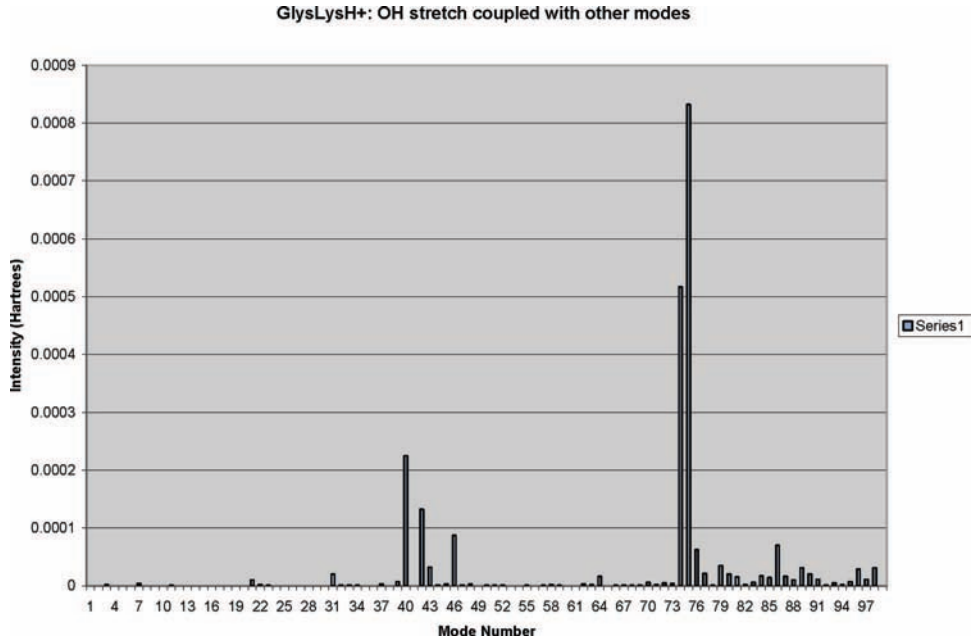

Figure 6. Graph showing integrated coupling potential between GlysLysH$^+$ OH stretch and other modes.

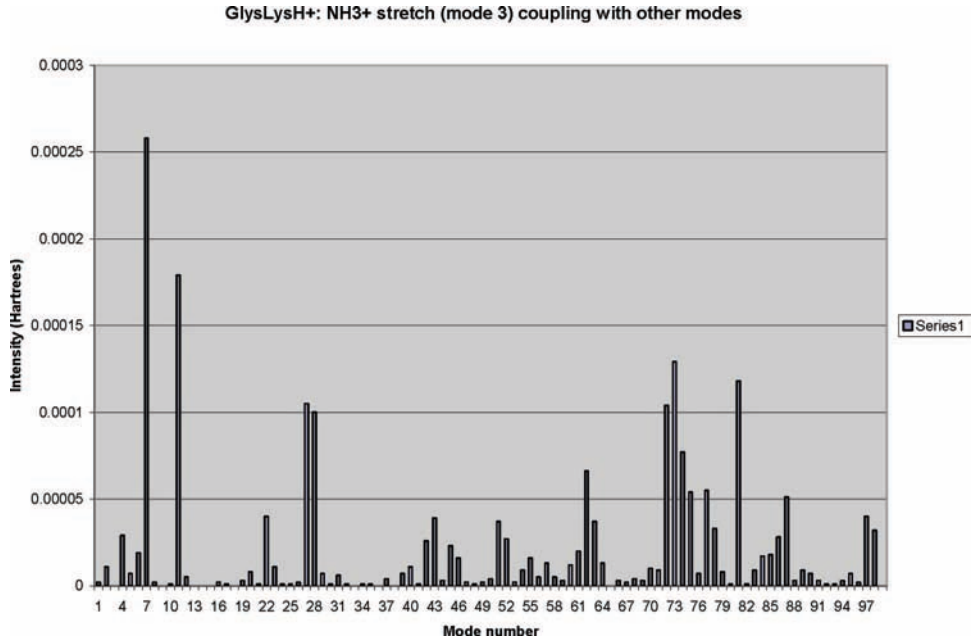

Figure 7. Graph showing integrated coupling potential between GlysLysH$^+$ and NH_3^+ (mode 3) and other modes.

most intense coupling is with modes 3 and 11, which are other NH_3^+ stretches (see Figure 8).

4. Concluding Remarks. In this paper, anharmonic vibrational spectroscopy calculations are carried out for two proton-bound amino acid complexes, GlysLysH$^+$ and GlyGlyH$^+$. The calculations use the CC-VSCF vibrational algorithm, and employed PM3 potentials, improved by fitting to ab initio MP2 data at the harmonic level of treatment. The results are compared with experiments for hydrogenic stretching transitions for which data is available. Several useful conclusions can be drawn: (1) Agreement between the calculated and observed frequencies is very good, being a substantial improvement over the ab initio harmonic results. The very close agreement with experiment supports the confidence in the structures of the protonated complexes which is also predicted by the calculations. The structures are the same as recently computed by ab initio calculations,[17] but the CC-VSCF calculations, when combined with the IRPD, provide experimental support. We are not aware of any direct determination of the structures of such systems. (2) The close agreement with experiment also validates the improved PM3 potentials used in the calculations. Reliable potentials for systems of this type are very necessary. Such an improved PM3 potential can be constructed and applied also for considerably larger protein-bound amino acids and peptides. It is certainly of great interest to apply such a potential, e.g. in molecular dynamics simulations. The formation of proton bridges between amino graphs was noted in a range of processes in charged proteins.[59] Such simulations could benefit from better potentials for protein bridge systems. (3) Some of the strong anharmonic effects found, though not all of them, are due to strong anharmonic coupling between different modes. This should be strongly related to vibrational energy flow in dynamics. A highly selective, "nondemocratic" pattern of mode−mode anharmonic coupling strength is found. It would

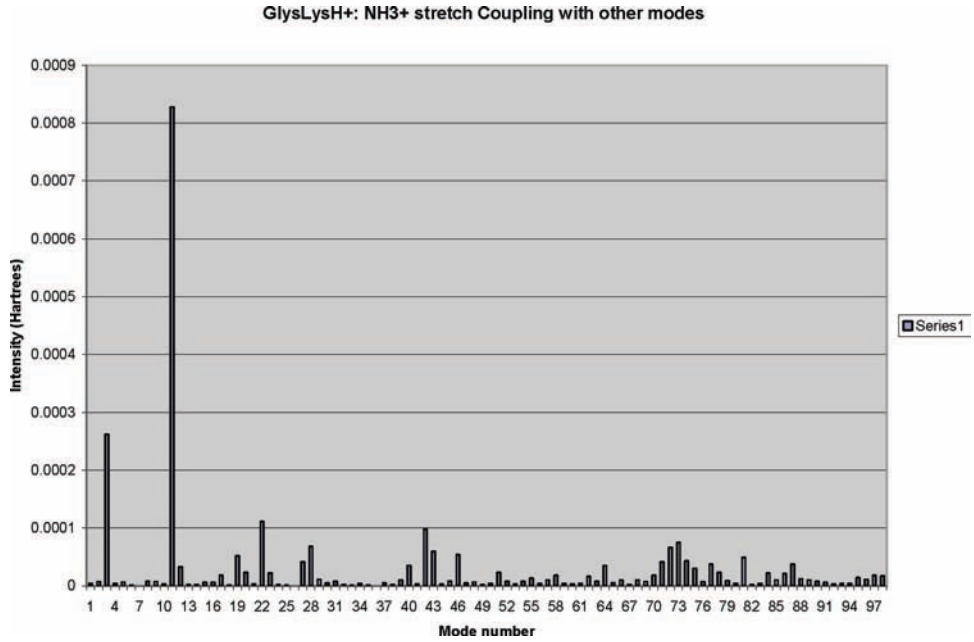

Figure 8. Graph showing integrated coupling potential between NH stretch mode 7 and other modes.

be of considerable interest in the future to explore the consequence of this for vibrational energy flow pathways in dynamics.We have calculated the anharmonic vibrational spectra of the proton bound amino acid wires, GlysLysH$^+$. The results from the and GlyGlyH$^+$. CC-VSCF calculations carried out on an *ab initio* improved PM3 surface provide a detailed view into anharmonicity and its accompanying effects in amino acid wires. The theoretical−experimental analysis shows that the explicit inclusion of anharmonic effects is very important for achieving agreement between theory and experiment as anharmonic frequencies obtained from

CC-VSCF calculations are of similarity to experiment. This agreement between theory and experiments validates the PES and encourages the use of high level ab initio methods not only in the theoretical spectroscopy of biological systems but also in applications such as molecular dynamics simulations. We also observe that with adequate scaling PM3 is indeed able to describe hydrogen-bonded complexes to a high degree of accuracy. This is important as PM3 is much faster than pure *ab initio* methods, and its efficient use will make the anharmonic treatment of large biological molecules possible.

In addition we have found that also intrinsic anharmonicities of single modes as well as coupled anharmonicities play an important role in proton bound amino acid wires. We have observed that the OH stretch in both GlysLysH$^+$ and GlysGlysH$^+$ is characterized mainly by intrinsic character while the NH_3^+ stretch generally has a more coupled anharmonic character. In this study we also characterized the coupling between different normal modes. The results show that the magnitude of anharmonic couplings between different pairs of normal modes depends very selectively on the modes involved. Vibrational energy transfer and redistribution in polyatomic molecules is due to anharmonic couplings between different modes. The findings on these couplings may hopefully motivate future experimental and theoretical studies on energy flow in these systems.

Acknowledgment. This paper is dedicated to Professor Max Wolfsberg, with thanks for helpful discussions on topics pertinent to this work. The research at The Hebrew University of Jerusalem was supported by the U.S−Israel Binational Science Foundation (BSF Grant 2004009).

References and Notes

(1) Chapo, C. J.; Paul, J. B.; Provencal, R. A.; Roth, K.; Saykally, R. J. *J. Am. Chem. Soc.* **1998**, *120*, 12956.
(2) Compagnon, I.; Oomens, J.; Bakker, J.; Meijer, G.; von Heldon, G. *Phys. Chem. Chem. Phys.* **2005**, *7*, 13.
(3) Dian, B. C.; Clarkson, J. R.; Zwier, T. S. *Science* **2004**, *303*, 1169.
(4) Dian, B. C.; Longarte, A.; Zwier, T. S. *Science* **2002**, *296*, 2369.
(5) Florio, G. M.; Zwier, T. S. *J. Phys. Chem. A* **2003**, *107*, 974.
(6) Rizzo, T. R.; Park, Y. D.; Levy, D. H. *J. Chem. Phys.* **1986**, *85*, 6945.
(7) Robertson, E. G.; Simons, J. P. *Phys. Chem. Chem. Phys.* **2001**, *3*, 1.
(8) Snoek, L. C.; Kroemer, R. T.; Hockridge, M. R.; Simons, J. P. *Phys. Chem. Chem. Phys.* **2001**, *3*, 1819.
(9) Crowe, M. C.; Brodbelt, J. S. *J. Am. Chem. Soc.* **2004**, *126*, 4786.
(10) Daneshfar, R.; Kitova, E. N.; Klassen, J. S. *J. Am. Chem. Soc.* **2004**, *126*, 4786.
(11) Fukui, K.; Naito, Y.; Akiyama, Y.; Takahashi, K. *Int. J. Mass Spectrom.* **2004**, *235*, 25.
(12) Jurchen, J. C.; Garcia, D. E.; Williams, E. R. *J. Am. Soc. Mass Spectrom.* **2003**, *14*, 1373.
(13) Jurchen, J. C.; Garcia, D. E.; Williams, E. R. *J. Am. Soc. Mass Spectrom.* **2004**, *15*, 1408.
(14) Meot-Ner, M. *J. Am. Chem. Soc.* **1974**, *96*, 3168.
(15) Choi, M. Y.; Miller, R. E. *J. Am. Chem. Soc.* **2006**, *128*, 7320.
(16) Choi, M. Y.; Douberly, G. E.; Falconer, T. M.; Lewis, W. K.; Kindsay, C. M.; Merritt, J. M.; Stiles, P. L.; Miller, R. E. *Int. Rev. Phys. Chem.* **2006**, *25*, 15.
(17) Oh, H.-B.; Lin, C.; Hwang, H. Y.; Carpenter, B. K.; McLafferty, F. W. *J. Am. Chem. Soc.* **2005**, *127*, 4076.
(18) Solca, N.; Dopfer, O. *Angew. Chem.* **2003**, *115*, 1575.
(19) Nir, E.; Kleinermanns, K.; de Vries, M. S. *Nature* **2000**, *408*, 949.
(20) Bakker, J. M.; Compagnon, I.; Meijer, G.; von Helden, G.; Kabelac, M.; Hobza, P.; de Vries, M. S. *Phys. Chem. Chem. Phys.* **2004**, *6*, 2810.
(21) Solca, N.; Dopfer, O. *Chem. Phys. Chem.* **2005**, *6*, 434.
(22) Compagnon, I.; Oomens, J.; Meijer, G.; von Helden, G. *J. Am. Chem. Soc.* **2006**, *128*, 3592.
(23) Chin, W.; Piuzzi, I. F.; Dimicolli, I.; Mons, M. *Phys. Chem. Chem. Phys.* **2006**, *8*, 1033.
(24) Bush, M. E.; O'Brien, J. T.; Prell, J. S.; Saykally, R. J.; William, E. R. *J. Am. Chem. Soc.* **2007**, *129*, 1612–1622.
(25) Simons, J. P. *Phys. Chem. Chem. Phys.* **2004**, *6*, E7.
(26) Snoek, L. C.; Robertson, E. G.; Kroemer, R. T.; Simons, J. P. *Chem. Phys. Lett.* **2000**, *321*, 49.
(27) Carcabal, P.; Kroemer, R. T.; Snoek, L. C.; Simons, J. P.; Bakker, J. M.; Compagnon, I.; Meijer, G.; von Helden, G. *Phys. Chem. Chem. Phys.* **2004**, *6*, 4546.

(28) Brauer, B.; Gerber, R. B.; Kabelac, M.; Hobza, P.; Bakker, J. M.; Abo-riziq, A. G.; de Vries, M. S. *J. Phys. Chem. A* **2005**, *109*, 6974.
(29) Abo-riziq, A.; Crews, B. O.; Callahan, M. P.; Grave, L.; de Vries, M. S. *Angew. Chem., Int Ed.* **2006**, *45*, 5166.
(30) Fenn, J. B.; Mann, M.; Meng, C. K.; Wong, S. F.; Whitehouse, C. M. *Science* **1989**, *246*, 264.
(31) Hillenkamp, F.; Karas, M.; Beavis, R.; Chait, B. *Anal. Chem.* **1991**, *63*, A1193.
(32) Oomens, J.; Von Helden, G.; Meijer, G. *J. Phys. Chem. A* **2004**, *108*, 8273.
(33) Lucas, G.; Gregoire, G.; Lemaire, J.; Maitre, P.; Glotin, F.; Scherman, G. P.; Desfrancois, G. *Int. J. Mass Spectrom.* **2005**, *243*, 105.
(34) Macleod, N. A.; Simons, J. P. *Phys. Chem. Chem. Phys.* **2004**, *6*, 2821–2826.
(35) Andrei, H.-S.; Solca, N.; Dopfer, O. *J. Phys. Chem.* **2005**, *109*, 3598.
(36) Solca, N.; Dopfer, O. *J. Am. Chem. Soc.* **2004**, *126*, 9520–9521, and references therein.
(37) Woo, C.-C.; Jiang, J. C.; Boo, D. W.; Lin, S. H.; Lee, Y. T.; Chang, H.-C. *J. Chem. Phys.* **2000**, *112*, 176–188.
(38) Wang, Y. S.; Tsai, C. H.; Lee, Y. T.; Chang, H.-C.; Jiang, J. C.; Asvany, O.; Schlemmer, S.; Gerlich, D. *J. Phys. Chem. A* **2003**, *107*, 4217–4225.
(39) Yeh, L. I.; Okumura, M.; Myers, J. D.; Price, J. M.; Lee, Y. T. *J. Chem. Phys.* **1989**, *91*, 7319–7330.
(40) Jiang, J.-Y.; Wang, Y.-S.; Chang, H.-C.; Lin, S. H.; Lee, Y. T.; Niedner-Schatterburg, G.; Chang, H.-C. *J. Am. Chem. Soc.* **2000**, *122*, 1398–1410.
(41) Price, W. D.; Schnier, P. D.; Williams, E. R. *J. Phys. Chem. B* **1997**, *101*, 664–673.
(42) Julian, R. R.; Hodyss, R.; Beauchamp, J. L. *J. Am. Chem. Soc.* **2001**, *123*, 3577–3583.
(43) Price, W. D.; Jockusch, R. A.; Williams, E. R. *J. Am. Chem. Soc.* **1997**, *119*, 11988–11989.
(44) Kapota, C.; Lemaire, J.; Matre, P.; Ohanessian, G. *J. Am. Chem. Soc.* **2004**, *126*, 1836–1847.
(45) Jung, J. O.; Gerber, R. B. *J. Phys. Chem.* **1996**, *105*, 10332–10348.
(46) Gregurick, S. K.; Chaban, G. M.; Gerber, R. B. *J. Phys. Chem. A* **2002**, *106*, 8696–8707.
(47) Brauer, G.; Chaban, G. M.; Gerber, R. B. *Phys. Chem. Chem. Phys.* **2004**, *6*, 2543–2556.
(48) Chaban, G. M.; Jung, J. O.; Gerber, R. B. *J. Phys. Chem.* **1999**, *111*, 1623–1629.
(49) Matsunaga, N.; Chaban, G. M.; Gerber, R. B. *J. Chem. Phys.* **2002**, *117*, Art. No. 3541.
(50) Adesokan, A. A.; Fredj, E.; Brown, E. C.; Gerber, R. B. *Mol. Phys.* **2005**, *103*, 1505–1520.
(51) Miller, Y.; Chaban, G. M.; Gerber, R. B. *J. Phys. Chem.* **2005**, *109*, 6565–6574.
(52) Benoit, D. M. *J. Phys. Chem.* **2004**, *120*, 562–573.
(53) Schmidt, M. W.; Baldridge, K. K.; Boatz, J. J.; Elbert, S. T.; Gordon, M. S.; Jensen, J. J.; Koseki, S.; Matsunaga, N.; Nguyen, K. A.; Su, S.; Windus, T. L.; Dupuis, M.; Montgomery, J. A. *J. Comput. Chem.* **1993**, *19*, 1347–1363.
(54) Bounouar, M.; Scheurer, C. *Chem. Phys.* **2008**, *347*, 194–207.
(55) Stewart, J. J. P. *J. Comput. Chem.* **1989**, *10*, 209–220.
(56) Bode, B. M.; Gordon, M. S. *J. Mol. Graphics Modell.* **1998**, *16*, 133–138.
(57) Dannenberg, J. J. *THEOCHEM* **1997**, *401*, 279–286.
(58) Leitner, D. *J. Phys. Chem. A* **1997**, *101*, 547–548.
(59) Steinberg, M. Z.; Breuker, K.; Elber, R.; Gerber, R. B. *Phys. Chem. Chem. Phys.* **2007**, *9*, 4690–4697.

JP807106H